18th IFHTSE CONGRESS
International Federation for Heat Treatment and Surface Engineering
IFHTSE
ANAIS
PROCEEDINGS
ISSN 1516-392X

METALLIC COATING ADHESION OBTAINED THROUGH THERMAL SPRAYING TESTING[1]

Rogério Varavallo[2]
Marcos Dorigão Manfrinato[3]
Luciana Sgarbi Rossino[4]
Flavio Camargo[5]
Omar Maluf[6]

Abstract
In order to study the metallic coating deposition obtained through High Velocity Oxygen Fuel (HVOF) thermal spraying process of the materials STELLIT 6 PM SD 38 EF, 97 MXC, 140 MXC, 1342 VM, 1350 VM and 8812, an adhesion testing device was built in accordance with ASTM C 633-79 standard. This standard is often used as a method of establishing the influence of spraying, the substrate's surface and the abrasive spray gun conditions, coating thickness, and other quality factors. Metallography, hardness and fracture surface analysis were performed. The fracture surface analysis revealed many results. In another words, they showed different fracture types: cohesive, adhesion and adhesive fracture.
Keywords: Thermal spraying; HVOF; Adhesion testing device.

ENSAIOS DE ADESÃO EM REVESTIMENTOS METÁLICOS OBTIDOS POR ASPERSÃO TÉRMICA

Resumo
Para estudo de processos de deposição de revestimentos metálicos obtidos através do processo de aspersão térmica chama combustível de alta velocidade (HVOF) dos materiais STELLIT 6 PM SD 38 EF, 97 MXC, 140 MXC, 1342 VM, 1350 VM e 8812, foi construído um dispositivo de ensaio de adesão através da norma ASTM C 633-79, usado freqüentemente como uma ferramenta para determinar a influência das condições de aspersão, da superfície do substrato e do jateamento abrasivo, espessura do revestimento, além de outros fatores da qualidade. Foi realizado ensaios de dureza, metalografia e análise da superfície de fratura. As análises das superfícies de fratura revelaram resultados variados, ou seja, apresentaram diferentes tipos de fratura: fraturas coesivas, aderência e fratura adesiva.
Palavras-chaves: Aspersão térmica; HVOF; Dispositivo para ensaio de aderência.

[1] *Technical contribution to the 18th IFHTSE Congress - International Federation for Heat Treatment and Surface Engineering, 2010 July 26-30th, Rio de Janeiro, RJ, Brazil.*
[2] *BA in Materials Science and Engeneering, EESC, São Paulo University, Brazil.*
[3] *MA in Materials Science and Engeneering Paulista Unip University, Brazil.*
[4] *PhD in Materials Science and Engeneering, EESC, São Paulo University, Brazil.*
[5] *Ogramac Indústria e Comércio Ltda,Santo Antônio da Posse - SP , Brazil.*
[6] *PhD in Materials Science and Engeneering, EESC, São Paulo University, Brazil.*

1 INTRODUCTION

Coatings are layers thicker than 10 μm, which can be applied through many methods: steam chemical and physical deposition; electrodeposition; soldering; clad; and thermal spraying.[1]

The use of protecting coatings applied through thermal spraying aims on decreasing the wear rates and increasing the resistance against the corrosion of materials, pieces and structure components.[2] The coatings are also used on pieces that need thermal and electric insulation. They have a wide range of applications because the material selection is nearly unlimited.[3,4]

The HVOF application method allows us to reach higher particle velocities when compared to the velocities of other systems like powder flame, ribbon flame, wire flame, detonation, electric arc, low-energy plasma and high-energy plasma.[5,6]

Through thermal spraying, the coating material, either as powder or wire, is melted by a chemical or electric heat source and boosted, by compressed air or other gases, against a previously prepared surface under cleanliness, topography (roughness) and temperature (heating) processes. The sprayed particles bond to the substrate by mechanical, chemical, metallurgic and physical nature mechanisms, depending on the temperature of the heat source and the velocity imposed to the particles, which form layers of lamellar structure interspersed with oxide inclusions and porosity made by the overlapping.

In the HVOF process, illustrated by Figure 1, the fuel gas is burned with high-pressure oxygen, generating a high velocity exhaustion jet. The fuel used can be propane, propylene, metal-acetylene-propane or hydrogen (most usual ones).[7] This fuel is mixed with the oxygen and burned inside a combustion chamber. The combustion products are liberated. Afterwards they expand through a nozzle, where the gas velocities become supersonic.[8] The powder is introduced into the nozzle, generally laterally; being heated and then accelerated outwards it. The combustion chamber and the nozzle are cooled on water.

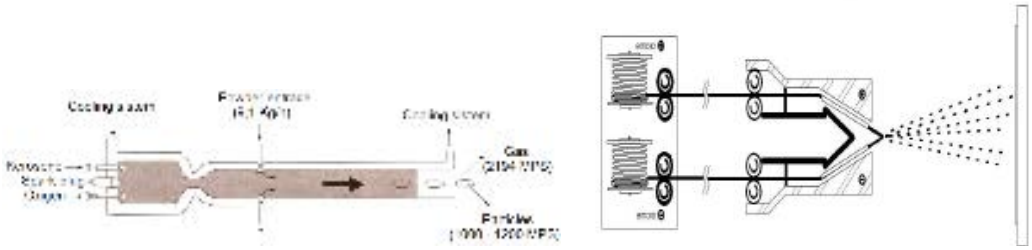

(a) (b)

Figure 1. Thermal spraying application process. (a) HVOF process. (b) Arc-Spray.

The AS (Arc-Spray) process, illustrated by Figure 1, uses an electric arc as the heat source to melt the deposition wire. The electric arc is obtained by a potential difference on the gun's nozzle, where two deposition material wires enter. A powerful jet of compressed air is aimed towards the electric arc in the part where the material gets molten, then atomizing and projecting it against the substrate. The activation of the continuous feed mechanism of the wire can be done by a little turbine that works with compressed air or electric motor. The projection velocity of the particles reaches 250 m/s.[9] The continuous current rectifier works between 18 and 40V and allows operating with many materials, pure or alloyed (solid or tubular). The wires form the opening of the strike arc and the size of the particles increases with the voltage

elevation. The voltage must be kept on the lowest levels to maintain the arc's stability. That should result on thicker and more uniform layers.

Although this process has been developed seeking an alternative to detonation spraying, it is also used nowadays as an option to plasma spraying in some applications. Besides the coating quality and lower residual stress, other advantages include deposit efficiency, lowered spraying angle sensitivity and less critical process variables.[10]

The aim of this work is to build an adhesion testing device and study the behavior and the influences of the spraying conditions, the surface of the substrate and abrasive spray gun, the coating thickness, as well as other quality factors related to adhesion of the substrate's sprayed layer.

2 MATERIALS AND METHODS

2.1 Machining of the Device and Specimens

Amongst the already existing standards, the chosen one for the adhesive resistance testing execution was the ASTM C 633-79, due to its lower cost and easy handling, which justify its wide use. Figure 2 illustrates the dimensions of the specimens used for the substrate deposit. They were made of 1020 steel, according to the adopted testing execution standard.[11] In order to build the device, it was used the 4340 steel, which went through a hardening temperature water after its machining, aiming the plug buckling avoidance during the testing.[12] The device and specimens' machining was performed in a universal Diplomat lathe model MS-220 Gold and a CNC Diplomat milling model PETRUS DPT-50100R.

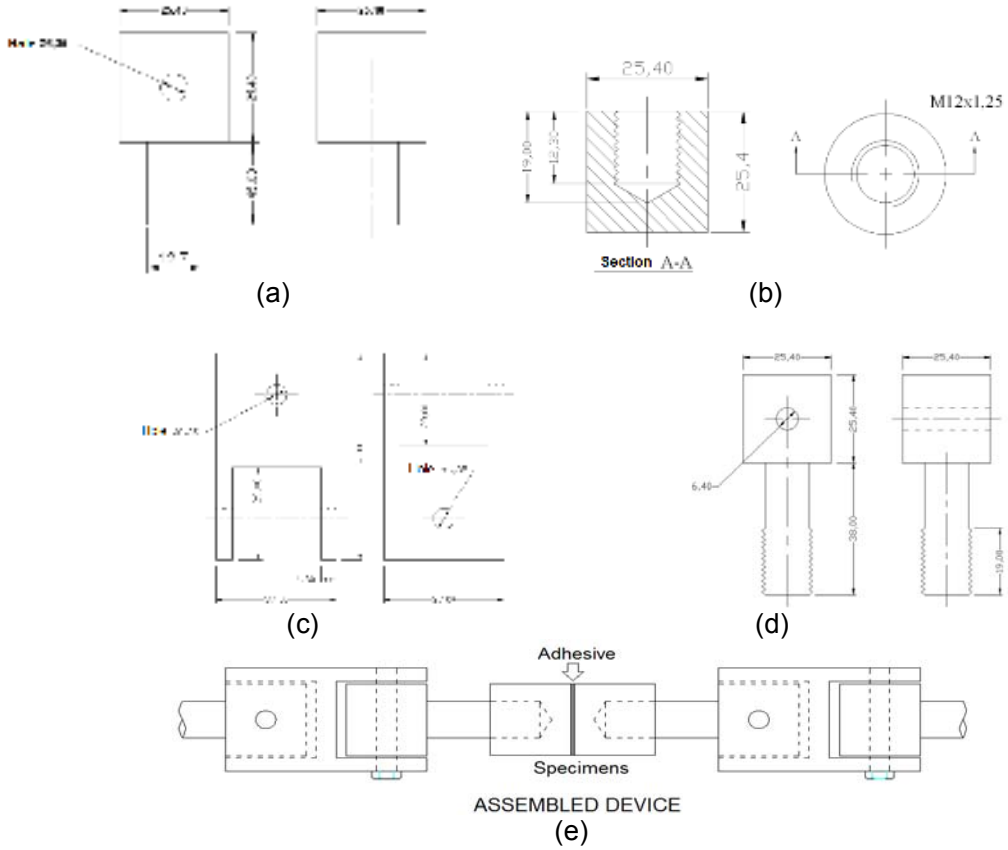

Figure 2. Traction testing device. (a) Body of the groove on the traction machine's claw and device groove. (b) Specimens' dimensions (c) Device body (d) Body of the device groove and thread for specimen attachment. (e) Assembled device, following the ASTM C 633-79 standard.

2.2 Thermal Spraying of the Specimens

After the machining of the specimens, their cleaning was done by a chemical process with a pickling acid and a degreaser. The surfaces of the specimens were mechanically cleaned (abrasive spray gun) using new aluminum oxide, alcohol and a dryer. Then the specimens were dried and taken to the performance of the spraying process. The specimens received the deposition of the following nanopowder materials, through the HVOF process: 1342 VM (81,83%WC-12,21%Co-5,5%C), 1350 VM (80,48%WC-10% Co-5,3%C) and 8812 (94,48%WC-11,56%Co-5,4%C) and, with tubular wire, through the Arc-Spray (AS) process: STELLIT 6 PM SD 38 EF (62,55% Co-29%Cr-4%W), 97 MXC (46,01%Fe-27,57%WC-13,32%Cr) and 140 MXC (60,48%Fe-15,9%Cr-7,07%W). Figure 3 illustrates the equipment working on the thermal spraying technique.

(a) (b)

Figure 3. Thermal spraying process in progress. (a) HVOF. (b) AS.

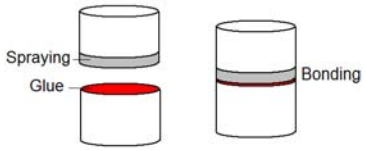

Figure 4. How the specimens were bonded with thermal spraying using the Scotch Weld DP-460 glue from 3M.

In order to do the adhesion testing, a specimen with spraying was bonded to another that wasn't sprayed, according to the Figure 4 illustration. The glue used for the bonding of the specimens was the Scotch Weld DP-460 from 3M. After the adhesive application, the specimens were taken to the adhesive curing oven. The adhesive curing temperature was 25°C during 100 hours, according to the manufacturer's specification.

2.3 Mechanical Testing of the Sprayed Layers

After the glue's curing, the adhesion testing was performed in an EMIC traction-testing machine at ambient temperature and a 2 mm/min strain velocity. The adhesion resistance limit values of the sprayed layers were fixed by the stress applied to the specimen when the breaking happens.

The (micro) Hardness Vickers (HV) Testing was done both on the sprayed layer and the matrix of the studied materials, using a Buehler 1600-6300 Microhardness Tester. The load used in the testing of all the samples was 100gf and the time of application of 15s, according to the ASTM E 384-99 standard. The reported surface hardness for each sample was the result of the average of seven impressions spread all over the sprayed layer for each type of sprayed layer studied in this work. The fracture surfaces of the studied specimens were observed using a stereoscope with image acquisition via camera with a resolution of 7.2 megapixels.

2.4 Roughness Testing

The surfaces of mechanical parts must be appropriate to the role they play. The roughness (micro geometric errors) is the set of irregularities, that is, small protrusions (spikes) and recesses (valleys) that characterize a surface, which influences on the sliding quality, wearing resistance, adjusting possibility of the forced coupling, resistance of the surface to the flow of fluids and lubricants, adhesion quality that the structure offers to the protecting layers, corrosion and fatigue resistance, sealing and appearance.[13] These irregularities can be evaluated with electronics, like the profilometer. Due to the material's surface quality importance, the specimens, after the spraying process, were tested for surface roughness, using a Mitutoyo SJ-201 profilometer, with Ra (average roughness) measurement unit and a CUT OFF of 0,8. Six surface measurements were made on different parts for each specimen.

3 RESULTS

3.1 Adhesion Testing of the Sprayed Layers

Figure 5 shows the device assembled to the traction machine. After the adhesion testing, in order to ease the changing of specimens, the plugs that attach the sample's attachment axle to the device body were removed.

The results of the sprayed specimens' adhesion testing 1342 VM, 1350 VM, 8812, STELLIT 6 PM SD 38 EF, 97 MXC, 140 MXC and the one with no thermal spraying are shown at Table 1.

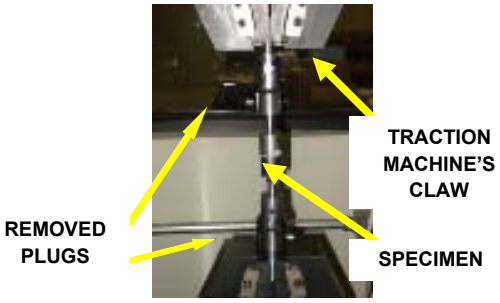

Figure 5. Adhesion testing device assembled to the traction machine.

Table 1. Adhesion limit values (MPa) of the glue and sprayed materials

	No Spraying	1342 VM	1350 VM	8812	STELLIT 6 PM SD 38 EF	97 MXC	140 MXC
	62,04	59,87	59,93	59,2	54,65	29,37	45,02
	61,32	60,39	56,82	59,2	55,02	29,37	44,98
	65,59	60,95	60,9	59,2	54,82	29,39	44,81
	63,78	60,65	60,5	59,2	55,56	29,39	44.91
	62,49	60,98	62,19	59,2	53,94	29,37	44,88
Average	63,04	60,57	60,07	59,2	54,8	29,37	44,92

3.2 Fractographic Analysis

On the adhesion tests done through the traction testing using adhesives, three types of fracture occur. They are classified according to the predominant place: adhesive (coating/substrate interface), cohesive (within the coating) and adhesive (within the adhesive or in its interfaces). These fracture types are detailed at Figure 6.

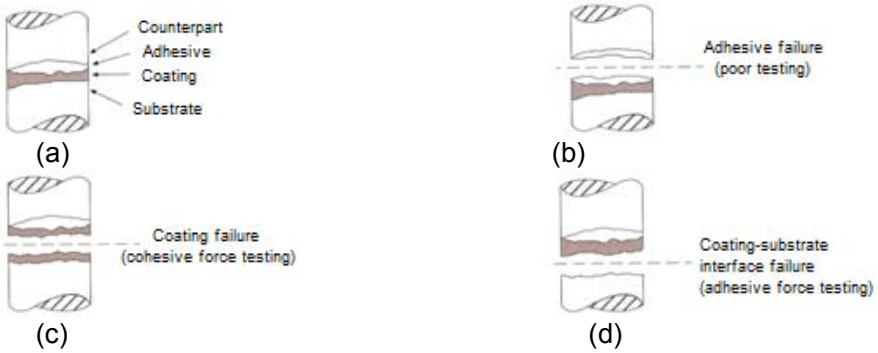

Figure 6. Fracture types resulting from the coating adhesion testing.

Figure 7 illustrates the topographies and fractures of the adhesion testing without thermal spraying and the materials STELLIT 6 PM SD 38 EF, 97 MXC, 140 MXC, 1342 VM, 1350 VM and 8812.

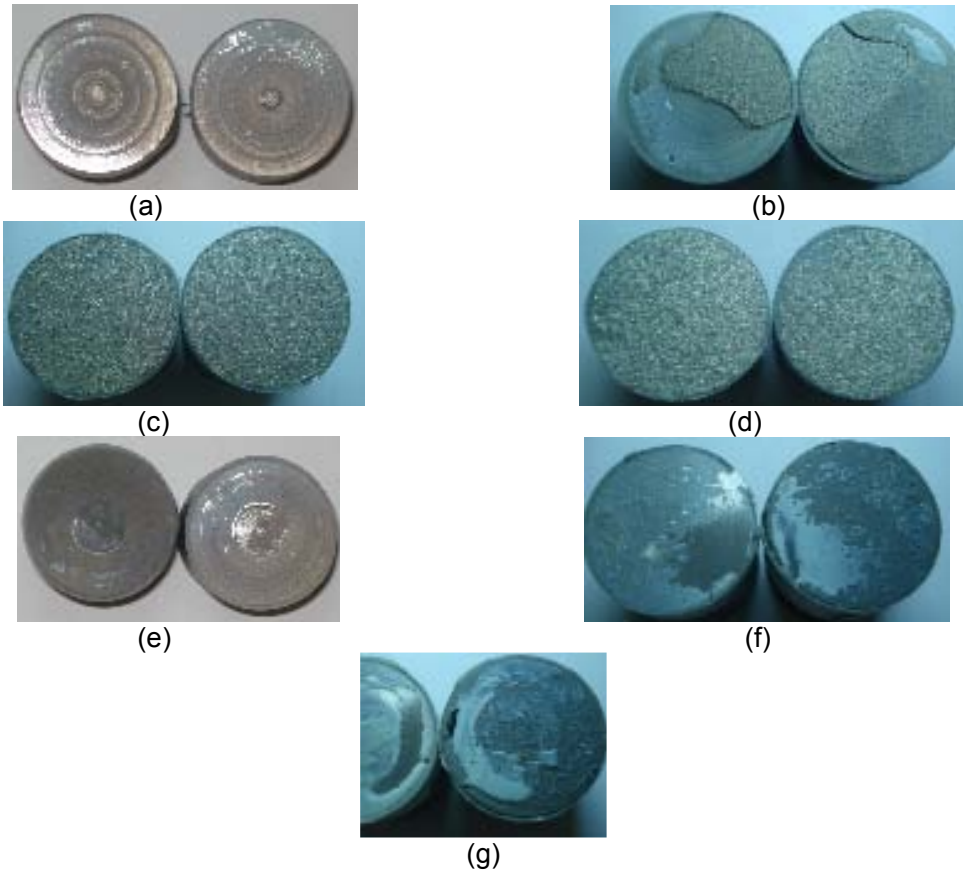

Figure 7. Fracture surface and macrographic aspects of the specimens' surfaces (a) without spraying and sprayed with (b) STELLIT 6 PM SD 38 EF (c) 97 MXC (d) 140 MXC (e) 1342 VM (f) 1350 VM (g) 8812.

The STELLIT 6 PM SD 38 EF sprayed layer showed cohesive failure determined by the detachment of the coating in half, and an adhesive failure that characterizes the removal of the coating from the substrate where it was applied. On the other hand, the 97 MXC and 140 MXC sprayed layers showed coating failure, characterizing cohesive force testing. The 1342 VM, 1350 VM and 8812 sprayed layers showed adhesive failure, which characterizes the disruption of the used glue.

3.2 Microhardness Testing and Roughness of the Sprayed Layers

Table 2 shows the results of microhardness testing done on the sprayed materials. Microhardness measurements were also performed at the base material of the specimens, AISI 1020 steel, whose average microhardness was 108 HV.

Table 2. Results of the microhardness measurements performed at the sprayed samples

Hardness Vickers (HV)						
Measurements	**STELLIT 6 PM SD 38 EF**	**1342 VM**	**1350 VM**	**8812**	**97 MXC**	**140 MXC**
1	659	864	824	1681	508	665
2	630	1354	946	1201	725	627
3	578	1056	946	1206	559	724
4	463	853	946	974	725	554
5	719	1064	1206	1168	824	559
6	592	1225	1206	980	846	664
7	706	1097	950	1190	761	626
Average	621 ± 87	1073 ± 180	1003 ± 145	1200 ± 235	707 ± 128	631± 60

Table 3 shows the obtained values of roughness of the studied sprayed layers.

Table 3. Roughness value of the specimens

ROUGHNESS VALUE (µm)						
	1342 VM	**1350 VM**	**STELLIT 6 PM SD 38 EF**	**8812**	**97 MXC**	**140 MXC**
	6,4	5,9	5,29	4,3	15,09	14,26
	6,27	6,3	6,5	5,85	13,03	12,62
	5,42	5,8	6,22	5,3	13,53	14,01
	7,1	6,8	6,02	6,05	14,41	12,41
	6,41	7,2	4,89	4,9	14,61	12,64
	5,7	6,3	5,22	5,7	14,78	14,09
Average	6,21	6,38	5,69	5,35	14,24	13,34

3.3 Metallography

Using the thermal spray gun, the studied materials were applied on the substrate, forming a lamellar structure with oxide inclusions, pores and empties, as shown at Figure 8. These structures are formed due to the distance between the substrate and the spray gun, the substrate temperature, the temperature in which the material is applied, air humidity, application velocity and types of applied materials. As seen at Figure 9 metallographies, the wire materials, STELLIT 6 PM SD 38 EF, 97 MXC and 140 MXC showed low porosity, empties, oxides and big lamellas. The nanopowder materials 1342 VM, 8812 and 1350 VM showed high porosity, oxides, small lamellas and low quantity of empties.

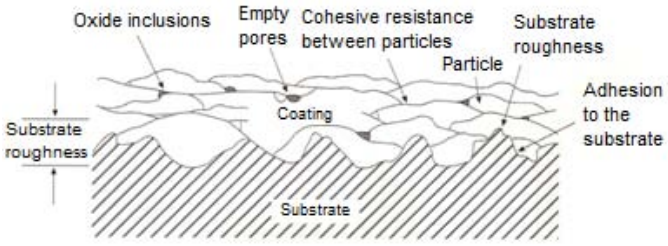

Figure 8. Lamellar structure of the sprayed layer.

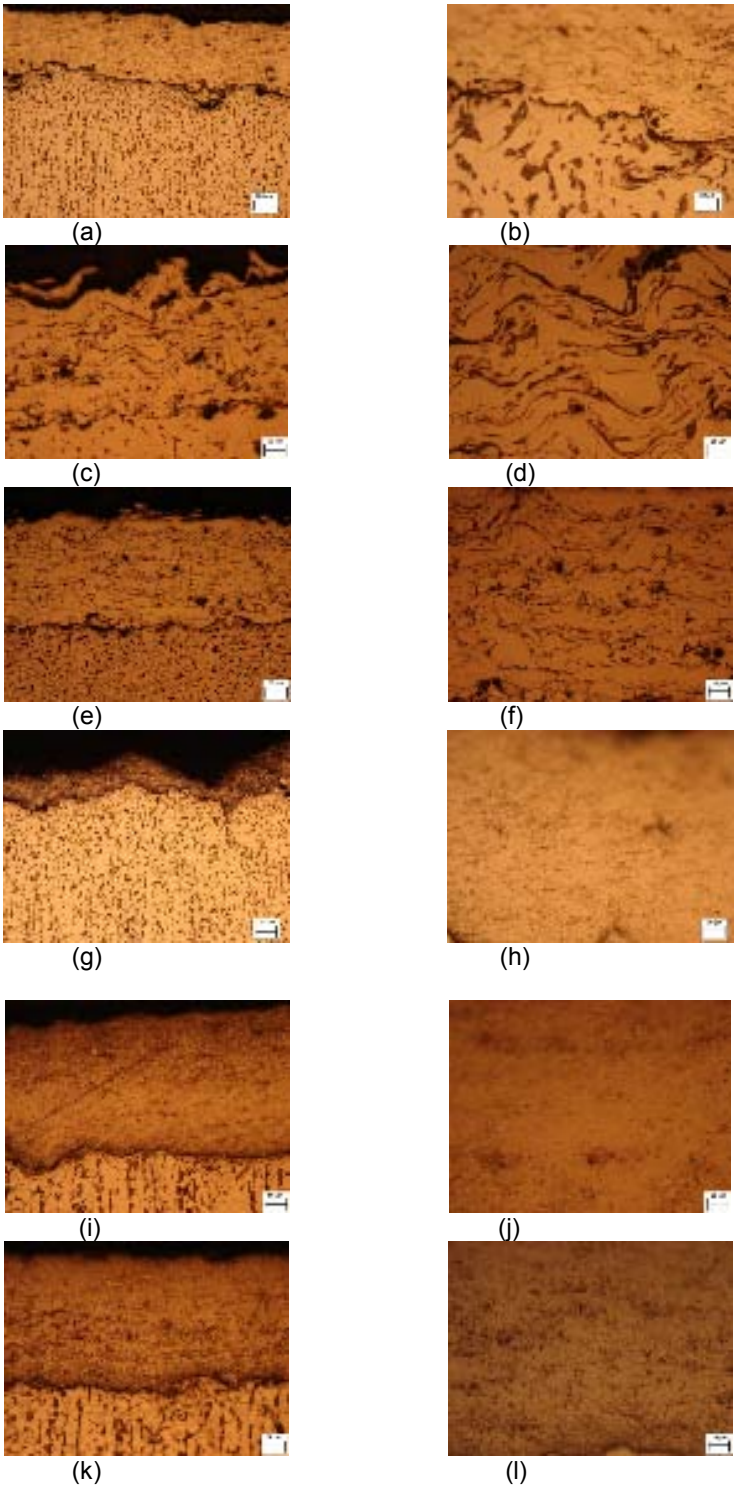

Figure 9. Metallography of the specimens deposited on the matrix material and attacked with Nital 2%. (a, b) STELLIT 6 PM SD 38 EF detail with a 10x and 500x zoom. (c, d) 97 MXC detail with a 200x and 500x zoom. (e, f) 140 MXC detail with a 200x and 500x zoom. (g, h) 1342 VM detail with a 10x and 500x zoom. (i, j) 8812 detail with a 200x and 500x zoom. (k, l) 1350 VM detail with a 200x and 500x zoom.

4 DISCUSSION

The microhardness values of the sprayed layer showed that they have high hardness when compared to the matrix material. However, the coatings deposited through wire (STELLIT 6 PM SD 38 EF, 97 MXC and 140 MXC) showed close microhardness amongst themselves, independent of the chemical composition, and inferior to the other coatings, given the formation of bigger grains in the deposited layers. The materials deposited through nanopowder (1342 VM, 1350 VM and 8812) showed higher microhardness, because their layers have very small grains and higher porosity than the ones deposited through wire, characterizing a more consistent bonding of the sprayed particles.

When nanopowder coatings (1342 VM, 1350 VM and 8812) were used, the average surface roughness found was 6 μm, but when wire coatings (STELLIT 6 PM SD 38 EF, 97 MXC e 140 MXC) were used, the average surface roughness found was 13,5 μm. This increase on the surface roughness when wire coatings are used is due to the formation of drops of molten material during the coating gun ignition process. These drops are bigger when compared to the molten nanopowder drops, which, when they reached the surfaces, form bumps and grooves causing an increase on the surface roughness of the sprayed layer.

When comparing the nanopowder and wire sprayed layers, porosity and grain's shape difference can be noted. For the nanopowder sprayed layers, 1350 VM, 1342 VM and 8812, we can see at Figure 8 (g, l) a high porosity. This porosity is due to the melting of the nanopowder materials during the HVOF process, which formed small liquid droplets that adhere to the layer making an opposition. The surface of these droplets oxidizes during the process. The dark spots on the Metallography represent this. For the STELLIT 6 PM SD 38 EF, 97 MXC and 140 MXC sprayed layers, we can see at Figure 8(a, f) the presence of a lower porosity. This low porosity is due to the formation of big droplets, with low velocity during the AS process.

The adhesion testing values of the specimen for the base material (without the sprayed layer) demonstrated that the 3M Scotch Weld DP-460 glue has, on average, an adhesion resistance of 63,04 Mpa, which will be a limiting factor to evaluate the coating type that has lower adhesion resistance when compared to the glue. For the coatings that show a higher adhesion limit, it is important to order the imported Scotch Weld EC-2214 glue by 3M, because it has a higher adhesion limit.

The fracture surface analysis of the specimens revealed the presence of three different types of failure, which are classified according to the predominant failure local: adhesive (coating-substrate interface), cohesive (within the coating) and adhesive (within the adhesive or in its interfaces).

Cohesive force testing occur due to imperfections on the sprayed layers like, for instance, gas bubbles confined between the coating layers, high coating porosity and thickness. The STELLIT, 97 MXC and 140 MXC materials showed these characteristics, because their coatings were fractured in half.

Adhesive force testing occur due to low adhesion, impurity, emptiness, dregs, low roughness and the way the coatings were applied to the substrates. The STELLIT material showed these characteristics, because its coating detached from the substrate.

The adhesive failure occurs due to the high adhesion value of these coatings in relation to the adhesion limit of the glue used in the testing. The 1342 VM, 1350 VM and 8812 materials showed these characteristics, because the glue didn't succeed on detaching the applied coatings, resulting on a poor testing.

The cohesive failures are not recommended if you want the layer to be efficient on its application. The variables that influence on this type of failure (cohesive) must be studied in order to eliminate this error from the process. One problem solving method would be the lowering of the layer thickness. The ideal layer thickness would be that one in which the fracture was adhesive. This work aimed on setting up testing systems in order to determine the adhesion resistance and understand the failure process of the sprayed layers. Later work must be developed in order to carry out a more detailed study about the spraying process efficiency and the pointing of the ideal parameters to produce sprayed layers with high adhesion resistance to the applied substrate.

Through the adhesive force testing it was found (on MPa) the average adhesion limit value of each layer. For the 1342 VM the value was 60,57 MPa, with an adhesive failure; for the 1350 VM the value was 60,07 MPa, resulting on an adhesive failure; on the other hand, for the STELLIT 6 PM SD 38 EF the value was 54,8 MPa, showing adhesive and cohesive failure; for the 97MXC the value was 29,37 MPa, showing cohesive failure; and for the 140 MXC the value was 44,92, showing cohesive failure. The adhesion of the layers applied through the HVOF process showed values that are related to the glue's adhesion, because with nanometric materials, supersonic velocities (800 to 1.200 m/s) and high application temperatures (2.900°C) there is a better anchoring, smaller size of the lamellas and high porosity, increasing then the material's hardness.

The materials applied through the Arc-Spray process showed lower values on the layer adhesion, because they were the wire type and their application velocity low (100 to 300 m/s) and application temperature (up to 5.000°C, depending on the fusion point of the materials) there is less anchoring, because they form bigger lamellas and higher porosity, reducing the material's hardness.

5 CONCLUSIONS

The built device showed constancy and no interference on the adhesion testing. Thus, it is able to perform a wide range of testing of layer adhesion to substrates.

For the 1342 VM, 1350 VM and 8812 sprayed coatings, it wasn't possible to determine the adhesion limit of these layers, because the glue used on the testing has a lower adhesion limit when compared to the coatings. The glue must be changed in order to perform the adhesion testing of these coatings. The glue that could be used is the Scotch Weld EC-2214 imported from the North-American 3M.

The layer characterization made possible the checking of the sprayed layers' behavior against the adhesion testing, and of the microhardness as well as the type of grain formed by each material. The layer deposited with wire coating (STELLIT 6 PM SD 38 EF, 97 MXC and 140 MXC) has lower microhardness when compared to the nanopowder applied coatings. This happens due to the size of the formed grain and the low porosity.

On the other hand, the nanopowder deposited layer (1342 VM, 1350 VM and 8812) showed higher hardness than the wire coating. This happens due to the small size of the grains and much higher porosity.

The STELLIT 6 PM SD 38 EF coating showed coating-substrate interface fracture, i. e. adhesive failure. It also showed cohesive failure, which was characterized by the layer fracture in half.

The 97 MXC and 140 MXC coatings showed cohesive fracture, i. e. the adhesion of the substrate particles ruptures.

In order not to let the cohesive failure happen, undesired at the layer resistance point of view, it is recommended doing a longer work so as to check the variables that can influence on the resistance of this type of layer, for instance using the substrate cleaning process, coating application and layer thickness.

Acknowledgements

I would like to express my appreciation to the company Ogramac Indústria e Comércio Ltda. for the production of all the research samples used in this study.

REFERENCES

1 Suganuma, k., Myiamoto, Y., Koizumi, M.; Joining of ceramic and metals, Annual, Review Materials Science, 1988, vol. 18.
2 Winkler, M. F., Parker, D. W.; Greener, maner diesels sport thermal barrier coatings, Advanced Materials and Processes, May 1992.
3 Lima,C.R.C. e Trevisan,R.E. “Aspersão Térmica – Fundamentos e Aplicações”. Artiliber Editora Ltda. 1 edição 2002.
4 American Welding Society, Thermal spraying – practice, theory and applications, Miami, FL, USA, 1985.
5 Tcker, R. C.; Thermal spray coatings, in ASM Handbook, vol. 5 – Surface Engineering, 1993.
6 Pawlowski, L.; The science and engineering of thermal spray coatings. John Wiley & Sons, New York, NY, 1995.
7 Parker, D. W.; Kutner, E. L.; HVOF spray technology poised for growth. Advanced Mateials and Processes, 1991, v. 139 (4).
8 Camargo, P. R. C.; brasagem a vacuo de metais dissimilares. Campinas: FEM, Unicamp, 1990. Tese (mestrado – Faculdade de Engenharia Mecânica, Universidade Estadual de Campinas, 1990.
9 Britton, C.R. 1988. Flame Spraying With Aluminium and Aluminium Alloys. Revista Aluminium Industry, vol 7/10, December.
10 Wigren, J.; Grit-blasting as surface preparation before plasma spraying. In: Proceedings of the National Thermal Spray Conference, Orlando, Florida, USA.
11 Berndt, C. C.; Leigh, S. H.; A test for coating adhesion on flat substrates – a technical note. Journal of Thermal spray Technology, vol. 3, nº2, June1994.
12 American Society for Testing and Materials - ASTM C 633 – 79. Standart Test Method for Adhesion or Cohesive Strength of Flame-Sprayed Coating.
13 Dias, J. S.; Motta, M. S.; Caracterização da Rugosidade Superficial Através da Técnica Ultra Sônica. Agosto 2002. Disponivel em: http://www.aaende.org.ar/sitio/biblioteca/material/PDF/COTE078.PDF. Acesso em: 14 Março 20010.